Carcinogenesis vol.30 no.7 pp.1115–1124, 2009
doi:10.1093/carcin/bgp105
Advance Access publication April 30, 2009

The isatin-Schiff base copper(II) complex Cu(isaepy)$_2$ acts as delocalized lipophilic cation, yields widespread mitochondrial oxidative damage and induces AMP-activated protein kinase-dependent apoptosis

Giuseppe Filomeni[1], Sara Piccirillo[2], Ilaria Graziani[1], Simone Cardaci[1], Ana M.Da Costa Ferreira[3], Giuseppe Rotilio[1,2] and Maria R.Ciriolo[1,2,*]

[1]Department of Biology, University of Rome ''Tor Vergata'', via della Ricerca Scientifica, 00133 Rome, Italy, [2]Research Centre IRCCS San Raffaele Pisana, Via dei Bonacolsi, 00163 Rome, Italy and [3]Departamento de Química Fundamental, Instituto de Química, Universidade de Sâo Paulo, PO Box 26077, CEP 05513-10 970, Sâo Paulo, SP, Brazil

*To whom correspondence should be addressed. Tel: +39 06 7259 4369; Fax: +39 06 7259 4311;
Email: ciriolo@bio.uniroma2.it

We previously demonstrated that Bis[(2-oxindol-3-ylimino)-2-(2-aminoethyl)pyridine-*N*,*N*′]copper(II) [Cu(isaepy)$_2$] was an efficient inducer of the apoptotic mitochondrial pathway. Here, we deeply dissect the mechanisms underlying the ability of Cu(isaepy)$_2$ to cause mitochondriotoxicity. In particular, we demonstrate that Cu(isaepy)$_2$ increases NADH-dependent oxygen consumption of isolated mitochondria and that this phenomenon is associated with oxy-radical production and insensitive to adenosine diphosphate. These data indicate that Cu(isaepy)$_2$ behaves as an uncoupler and this property is also confirmed in cell systems. Particularly, SH-SY5Y cells show: (i) an early loss of mitochondrial transmembrane potential; (ii) a decrease in the expression levels of respiratory complex components and (iii) a significant adenosine triphosphate (ATP) decrement. The causative energetic impairment mediated by Cu(isaepy)$_2$ in apoptosis is confirmed by experiments carried out with ρ^0 cells, or by glucose supplementation, where cell death is significantly inhibited. Moreover, gastric and cervix carcinoma AGS and HeLa cells, which rely most of their ATP production on oxidative phosphorylation, show a marked sensitivity toward Cu(isaepy)$_2$. Adenosine monophosphate-activated protein kinase (AMPK), which is activated by events increasing the adenosine monophosphate:ATP ratio, is deeply involved in the apoptotic process because the overexpression of its dominant/negative form completely abolishes cell death. Upon glucose supplementation, AMPK is not activated, confirming its role as fuel-sensing enzyme that positively responds to Cu(isaepy)$_2$-mediated energetic impairment by committing cells to apoptosis. Overall, data obtained indicate that Cu(isaepy)$_2$ behaves as delocalized lipophilic cation and induces mitochondrial-sited reactive oxygen species production. This event results in mitochondrial dysfunction and ATP decrease, which in turn triggers AMPK-dependent apoptosis.

Introduction

In the last years, new chemotherapeutic approaches have been developed in order to increase the selective killing of tumor cells. Therefore, besides conventional drugs mainly aimed at affecting DNA replication of rapidly dividing tumor cells, new molecules targeting other cellular compartments crucial for tumor cell survival have been tested.

Mitochondria are essential to provide adenosine triphosphate (ATP) for all cellular endoergonic processes and recently have been recognized as integrators of intrinsic and extrinsic apoptotic pathways. Electrons from reducing equivalents are funneled through the mitochondrial respiratory chain complexes to finally reduce oxygen. The transport of electrons is coupled to proton pumping into the intermembrane space resulting in the characteristic negative proton electrochemical gradient across the mitochondrial inner membrane. The free energy accumulated in the proton gradient is used to generate ATP.

Cancer cells need a higher amount of energy supply to sustain their faster rate of growth and proliferation. This requirement leads to a different energy metabolism (frequently glycolysis increase) that allows cancer cells surviving even in restrictive conditions, such as hypoxia (1). Therefore, compounds causing ATP depletion, such as inhibitors of glycolysis and/or oxidative phosphorylation (2–4), have been exploited as inducers of cell death in tumors (5). Among the molecules that are able to affect cellular energetics, delocalized lipophilic cations (DLCs) are considered as a promising class of compounds since, due to their positive charge, they selectively target mitochondria. In fact, the difference between plasma membrane potential ($\Delta\Psi_p$) and mitochondrial transmembrane potential ($\Delta\Psi_m$), which is about −120 mV, allows DLCs to be 100-fold more concentrated within mitochondria with respect to the cytosol (6). The $\Delta\Psi_m$ can vary among metabolic status of the cell and among different cell types (7), tumor carcinoma cells often being among those with higher mitochondrial membrane potential. The intrinsic variation of the $\Delta\Psi_m$ among cell types and the crucial role of this parameter in mitochondrial homeostasis provide a unique opportunity for selective drug accumulation into tumor cells with potential therapeutic effect. In fact, earlier studies have shown that the constitutively higher $\Delta\Psi_m$ of transformed cells could be used to selectively target toxic DLCs that accumulate in their mitochondria in response to $\Delta\Psi_m$. The mechanisms of DLCs-induced mitochondriotoxicity are varied, but all converging on the impairment of oxidative phosphorylation process, either by inhibiting F_0F_1-ATPase, as demonstrated for rhodamine 123 and the thiopyrilium AA-1 (2,8,9), or by affecting other components of the electron transfer chain. Dequalinium chloride and certain thiocarbocyanines have been indicated to inhibit NADH: ubiquinone oxidoreductase activity of mitochondrial Complex I (6,10,11), whereas the rhodocyanine MKT-077 yields a widespread mitochondrial dysfunction by inhibiting the activity of membrane-bound respiratory enzymes (6,12,13). However, regardless of their mechanism of action, DLCs give rise to an impairment of ATP synthesis and, consequently, a rapid decrement of its intracellular levels.

We previously characterized the proapoptotic activity of isatin-Schiff base copper(II) complexes, and we demonstrated that the Bis[(2-oxindol-3-ylimino)-2-(2-aminoethyl)pyridine-*N*,*N*′]copper(II), named Cu(isaepy)$_2$, was highly efficient in the induction of death in neuroblastoma cells (14). We also provide clear-cut evidence that this copper complex induced damage to specific cellular compartments, thus inducing programmed cell death through the mitochondrial pathway. Indeed, the positive charge of the complex and the preferential accumulation of copper within the mitochondrial compartment allowed us to suggest a role for Cu(isaepy)$_2$ as DLC-like molecule.

In this study, we dissected the mechanisms underlying the mitochondriotoxic activity of Cu(isaepy)$_2$, providing evidence for a preferential impairment of Complex I of the electron transport chain and the mitochondrial NADH:quinone oxidoreductases as the preferential site for reactive oxygen species (ROS) production. Moreover, adenosine monophosphate-activated protein kinase (AMPK) was found to be implicated in the molecular mechanisms linking the energetic impairment to the induction of apoptosis.

Abbreviations: ADP, adenosine diphosphate; AMPK, adenosine monophosphate-activated protein kinase; ATP, adenosine triphosphate; DLC, delocalized lipophilic cation; ROS, reactive oxygen species.

Materials and methods

Materials

Isatin-diimine copper(II) complex Bis[(2-oxindol-3-ylimino)-2-(2-aminoethyl)pyridine-*N*,*N*′]copper(II) perchlorate, $[Cu(isaepy)_2](ClO_4)_2$, named Cu (isaepy)2, was synthesized as described previously (14). The analogous isatin-imine zinc(II) complex $[Zn(isaepy)Cl_2]$, designated as Zn(isaepy), was prepared similarly using zinc chloride to metalate *in situ* the isaepy ligand (supplementary Figure 1 is available at *Carcinogenesis* Online). Antimycin A, catalase, dimethyl sulfoxide, dithiothreitol, ethylenediaminetetraacetic acid, ethidium bromide, ethylene glycol tetraacetic acid, glucose, paraformaldehyde, propidium iodide, rotenone, sodium pyruvate and Triton X-100 were from Sigma (St Louis, MO). Goat anti-mouse IgG (H+L)–horseradish peroxidase conjugate was from Bio-Rad Laboratories (Hercules, CA). *N*-Tris (hydroxymethyl)methyl-2-aminoethanesulfonic acid was from US Biological (Cleveland, OH). All other chemicals were from Merck (Darmstadt, Germany).

Cell culture

Human neuroblastoma SH-SY5Y, cervix carcinoma HeLa and gastric adenocarcinoma AGS cells were grown in Dulbecco's modified Eagle's medium/F12, Dulbecco's modified Eagle's medium and F12, respectively, supplemented with 10% fetal calf serum, glutamine and penicillin/streptomycin. Cells were cultured at 37°C in an atmosphere of 5% CO_2 in air. During the experiments cells were plated at a density of $4 \times 10^4/cm^2$, unless otherwise indicated.

For the generation of a stable ρ^0 line, SH-SY5Y cells were grown in 5 μg/ml ethidium bromide for two months (15), at the end of which they were analyzed for the loss of mitochondrial DNA, as well as cytochrome *c* oxidase activity.

Cells were transiently transfected by electroporation using a GenePulser xcell system (Bio-Rad Laboratories) according to the manufacturer's instructions. Transfections were performed with a pcDNA3 empty vector or with a pcDNA3 vector containing the myc-tagged coding sequence for the α2 subunit of AMPK carrying the T→A substitution at the residue 172 (kindly provided by Prof. David Carling from the Clinical Sciences Centre, Imperial College, Hammersmith Hospital, Du Cane Road, London, UK). After transfection, cells were immediately seeded into fresh medium and used after 48 h since this time was sufficient to significantly increase the expression of this dominant/negative form of AMPK.

Treatments

A 5 mM solution of $Cu(isaepy)_2$ or Zn(isaepy) was prepared just before the experiments by dissolving the lyophilized compounds in dimethyl sulfoxide. Treatments were performed in serum-supplemented media with $Cu(isaepy)_2$ or Zn(isaepy) at the final concentration of 50 μM for SH-SY5Y and 10 μM for AGS or HeLa.

Glucose and sodium pyruvate were added to the medium to reach the final concentration of 30 and 10 mM, respectively.

Proteasome inhibitor MG132, at the concentration of 10 μM, was added to the medium and maintained throughout the experiments.

Cell viability

Cell viability was estimated by direct count upon Trypan blue exclusion. For the evaluation of apoptosis, cells were stained with 50 μg/ml propidium iodide prior to analysis by a FACScalibur instrument (BD Biosciences, San José, CA). The percentages of apoptotic cells were evaluated as described previously (14). Alternatively, cells were counted upon Trypan blue staining by optic microscopy.

Cell growth was assessed by CellTiter 96® AQueous Cell Proliferation Assay kit (Promega, Madison, WI). After 24 h of treatment with $Cu(isaepy)_2$ or Zn(isaepy), cell were washed, replaced with fresh medium containing 3-(4,5-dimethylthiazol-2-yl)-5-(3-carboxymethoxyphenyl)-2-(4-sulfophenyl)-2H-tetrazolium inner salt (1:10 vol/vol) and incubated for 2 h in the dark. Absorbance at 490 nm was considered proportional to cell number.

$\Delta\Psi_m$ measurement

$\Delta\Psi_m$ was analyzed taking advantage of the $\Delta\Psi_m$-sensitive probe MitoTracker Red® (Invitrogen–Molecular Probes, San Giuliano Milanese, Italy) by fluorescence microscopy or cytofluorometrically. In the first case, cells were seeded on chamber slides at $6 \times 10^4/cm^2$ and treated for 6 h with $Cu(isaepy)_2$. At the end of the treatment, they were stained with 50 nM of MitoTracker Red® in combination with an anti-Hsp60 antibody (Santa Cruz Biotechnology, Santa Cruz, CA), washed and fixed with 4% paraformaldehyde. Images of cells were acquired and digitized with a Delta Vision Restoration Microscopy System (Applied Precision, Issaquah, WA) equipped with an Olympus IX70 fluorescence microscope. Alternatively, after 6 and 12 h of treatment, cells were incubated with 50 nM of MitoTracker Red® for further 30 min, washed, trypsinized, resuspended in phosphate-buffered saline and cytofluorometrically analyzed.

Cell fractionation and oxygen consumption

Mitochondria from mouse liver were obtained by mincing the hepatic tissue with three volumes (wt/vol) of 10 mM Tris–HCl, pH 7.5, 15 mM $MgCl_2$, 10 mM KCl and protease inhibitor cocktail. After 15 min on ice, equal volumes of 400 mM sucrose, 10 mM *N*-Tris(hydroxymethyl)methyl-2-aminoethanesulfonic acid, 0.1 mM ethylene glycol tetraacetic acid and 2 μM dithiothreitol, pH 7.2 were added and tissue disrupted by 40 strokes in a glass Dounce. Mitochondria-containing supernatants, obtained after centrifugation of lysates at 900*g* for 10 min, were further centrifuged at 12 000*g* for 15 min to finally separate mitochondria (pellet) from the cytosol (supernatant).

Oxygen consumption was determined at 25°C using a Clark-type oxygen electrode equipped with thermostatic control and magnetic stirring. Mitochondria were resuspended in 1.5 ml of 'experimental' buffer (125 mM KCl, 10 mM Tris–3-(N-morpholino)propane sulfonic acid, pH 7.4, 10 μM ethylene glycol tetraacetic acid–Tris, pH 7.4, 5 mM glutamate, 2.5 mM malate, 1 mM K_2HPO_4). NADH was added at final concentration of 1 mM in the presence or absence of 50 μM $Cu(isaepy)_2$. Rotenone and antimycin A were used at the final concentration of 5 μM, whereas KCN at 1 mM. Catalase was added to the experimental buffer at the concentration of 0.5 U. Before each analysis, as well as in the evaluation of P:O ratio upon incubations with $Cu(isaepy)_2$, state III:state IV ratio was measured by adding adenosine diphosphate (ADP; 0.2 μmol) to check the goodness of mitochondrial fraction.

Western blot analyses

Total lysates and mitochondrial-enriched fraction from SH-SY5Y cells were obtained as described previously (14). Proteins were electrophoresed by sodium dodecyl sulfate–polyacrylamide gel electrophoresis and blotted onto polyvinylidene difluoride membrane (Bio-Rad Laboratories). Monoclonal anti-subunit II of cytochrome *c* oxidase, anti-39 kDa subunit of Complex I (Invitrogen–Molecular Probes) and anti-Hsp60 (Santa Cruz Biotechnology) were used on blotting from mitochondrial fraction. Anti-SOD1 and anti-Hsp60 (Santa Cruz Biotechnology) were used as loading/purity control of cytosolic and mitochondrial fractions, respectively. Polyclonal anti-caspase-9 (Cell Signaling Technology, Beverly, MA), anti-c-myc and anti-glyceraldehyde-3-phosphate dehydrogenase (Santa Cruz Biotechnology) and monoclonal anti-phospho-thr172 of AMPK α-subunits, anti-caspase-3 (Cell Signaling Technology), anti-poly(ADP-ribose) polymerase and anti-AMPK (Santa Cruz Biotechnology) were used on total cell lysates as primary antibodies. The protein complex, formed upon the reaction with specific secondary antibodies, was identified using a FluorChem Imaging System (Alpha Innotech, M-Medical, Italy) after the incubation with ChemiGlow chemoluminescence substrate (Alpha Innotech). Densitometry was performed using Quantity One Software (Bio-Rad Laboratories).

Protein carbonyls detection

Carbonylated proteins were detected using the Oxyblot Kit (Intergen, Purchase, NY) on cytosolic and mitochondrial fractions. Briefly, 10 μg of mitochondrial proteins and 25 μg of cytosolic proteins were reacted with 2,4-dinitrophenylhydrazine for 15 min at 25°C. Samples were resolved on 8.5% sodium dodecyl sulfate–polyacrylamide gel electrophoresis and 2,4-dinitrophenylhydrazone-derivatized proteins were identified by immunoblot using an anti-2,4-dinitrophenylhydrazone antibody. Densitometry was performed using Quantity One Software and normalized to the amount of protein loaded.

ATP measurement

Cells were lysed and incubated in 100 mM Tris–HCl, 4 mM ethylenediaminetetraacetic acid, pH 7.75 for 2 min at 100°C. ATP levels were then measured by the ATP Bioluminescence Assay Kit CLS II (Roche Applied Science, Milan, Italy) using a microplate luminometer (Perkin Elmer, Milan, Italy) after incubation with the luciferin/luciferase reagents.

Protein determination

Proteins were determined by the method of Lowry *et al.* (16).

Data presentation

All experiments were done at least five different times unless otherwise indicated. The results are presented as means ± SDs. Statistical evaluation was conducted by analysis of variance, followed by correction with Bonferroni's test. Comparisons were considered to be significant at $P < 0.05$.

Results

$Cu(isaepy)_2$ oxidatively affects mitochondria of SH-SY5Y cells

Previously, we demonstrated that SH-SY5Y cells treated with Cu $(isaepy)_2$ underwent apoptosis through the activation of the mitochondrial route (14). Such phenomenon correlated with an accumulation of

copper within the nucleus and mitochondria, which represented the cell compartments particularly affected by Cu(isaepy)$_2$. Here, to assess the involvement of mitochondrial dysfunction as causative of apoptosis, we treated SH-SY5Y cells with 50 μM Cu(isaepy)$_2$ for 6 h and evaluated mitochondrial network by fluorescence microscopy. Figure 1A shows images obtained by means of double staining with MitoTracker Red and Hsp60-specific antibody. Upon treatment with Cu(isaepy)$_2$, mitochondria appeared isolated and organized as dotted or fragmented, features predictive of mitochondrial fission and removal (17). Moreover, MitoTracker Red staining indicated that only few mitochondria maintained unaltered their $\Delta\Psi_m$. In contrast, only slight effects were visible when the cells were treated with Zn(isaepy), an analogous of Cu(isaepy)$_2$, in which zinc, a non-redox active metal ion, replaced copper in the complex (14). In fact, mitochondria maintained their reticular organization and $\Delta\Psi_m$, confirming that copper was indispensable for Cu(isaepy)$_2$-induced mitocondriotoxicity. Nevertheless, incubations with the zinc complex significantly affected $\Delta\Psi_m$ at longer time points (i.e. 12 h, Figure 1B). Therefore, we performed dose-response experiments and an IC_{50} (the concentration that gives 50% inhibition of cellular growth) of ~350 μM for Zn(isaepy) with respect to 30 μM for Cu(isaepy)$_2$ was determined (supplementary Figure 2A is available at *Carcinogenesis* Online), confirming the high efficacy of Cu in inducing cytotoxicity. However, since free copper can theoretically displace zinc from Zn(isaepy) to generate Cu(isaepy) and Cu(isaepy)$_2$, we carried out exchange kinetics experiments and we found that copper, actually, displaced zinc from the complex in phosphate buffer ($K_{eq} = 3.72 \times 10^{-4}$, supplementary Figure 2B and C is available at *Carcinogenesis* Online). These data, together with the

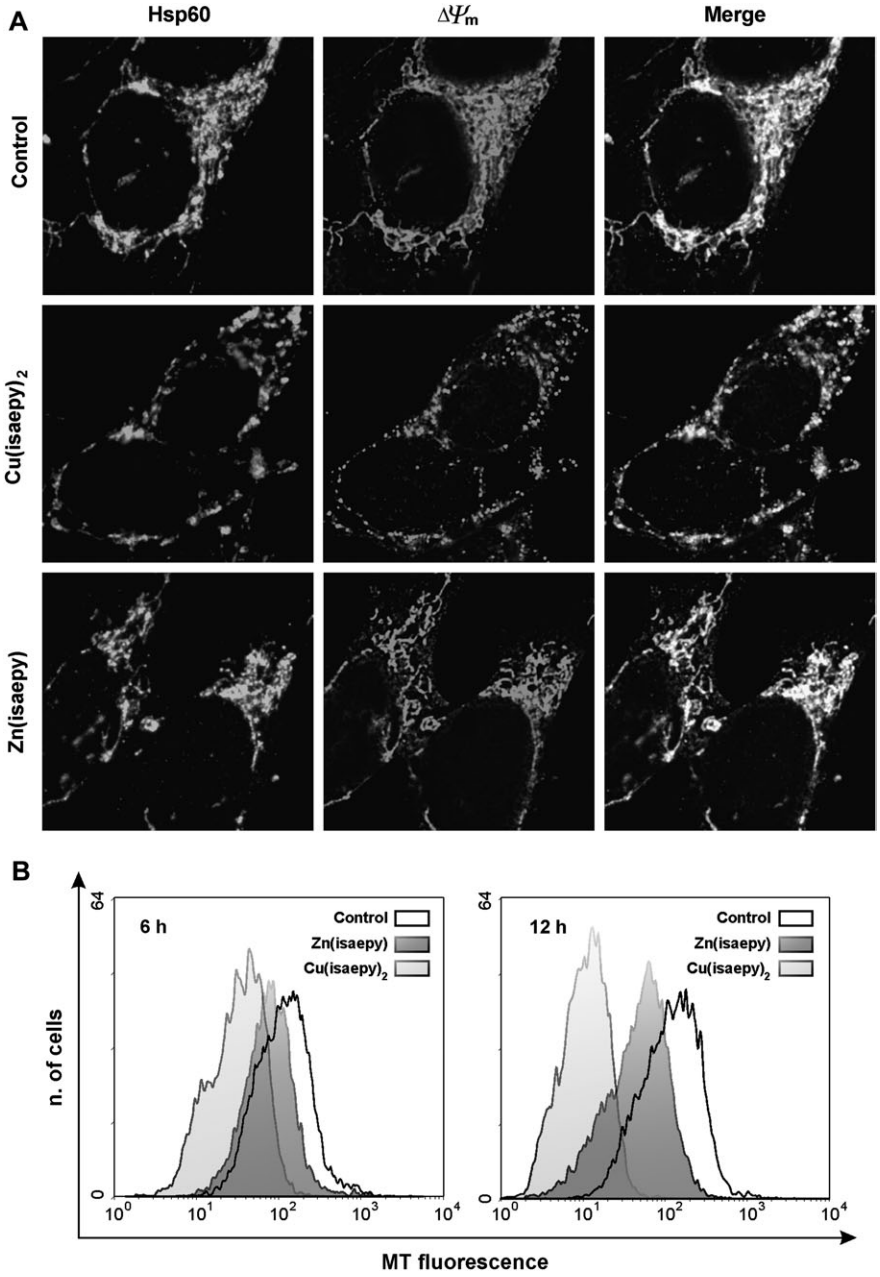

Fig. 1. Effect of Cu(isaepy)$_2$ on mitochondrial network. (**A**) SH-SY5Y cells were grown on chamber slides and treated for 6 h with 50 μM Cu(isaepy)$_2$ or Zn(isaepy). Before fixation, cells were incubated for 30 min with 50 nM MitoTracker Red® and subsequently probed with an anti-Hsp60 specific antibody. Images of cells were digitized with a Delta Vision Restoration Microscopy System equipped with an Olympus IX70 fluorescence microscope. (**B**) SH-SY5Y cells were treated for 6 and 12 h with 50 μM Cu(isaepy)$_2$ or Zn(isaepy), incubated for 30 min with 50 nM MitoTracker Red (MT) and cytofluorometrically analyzed for $\Delta\Psi_m$ by FACScalibur instruments. Histograms shown are representative of three independent experiments that gave similar results.

knowledge that free copper is virtually not available *in vivo* (18), allow us to suggest that Zn(isaepy) is toxic only at very high concentrations, even though we cannot exclude the possibility that part of its toxicity could be due to copper displacement.

To investigate whether mitochondrial damage was due to mitochondrial electron transfer chain impairment, we analyzed by western blot analysis the expression levels of Complex I and IV. Figure 2A shows that subunit II of cytochrome *c* oxidase was significantly reduced already after 6 h of treatment, reaching 50% decrement after 12 h. The 39 kDa subunit of Complex I was also affected by $Cu(isaepy)_2$ treatment, although to a lesser extent (−30% after 12 h), whereas no change in the levels of both proteins were observed upon treatment with Zn(isaepy). Therefore, to assess alterations in mitochondrial function, ATP content was measured in SH-SY5Y cells. Figure 2B shows that ATP decreased significantly in a time-dependent manner, starting from 6 h and reaching >50% decrement after 24 h treatment with $Cu(isaepy)_2$.

Mitochondria are the major intracellular source of ROS, which are more abundant in response to mitochondrial dysfunction. We therefore measured the level of protein carbonyls, as by-products of ROS-mediated damage, both on cytosolic- and mitochondrial-enriched fractions. Figure 2C shows that $Cu(isaepy)_2$ yielded a very early and higher increase in carbonyl levels than Zn(isaepy), in both fractions. Moreover, the trend of accumulation of the oxidized proteins was completely different, with a time-dependent increase in the

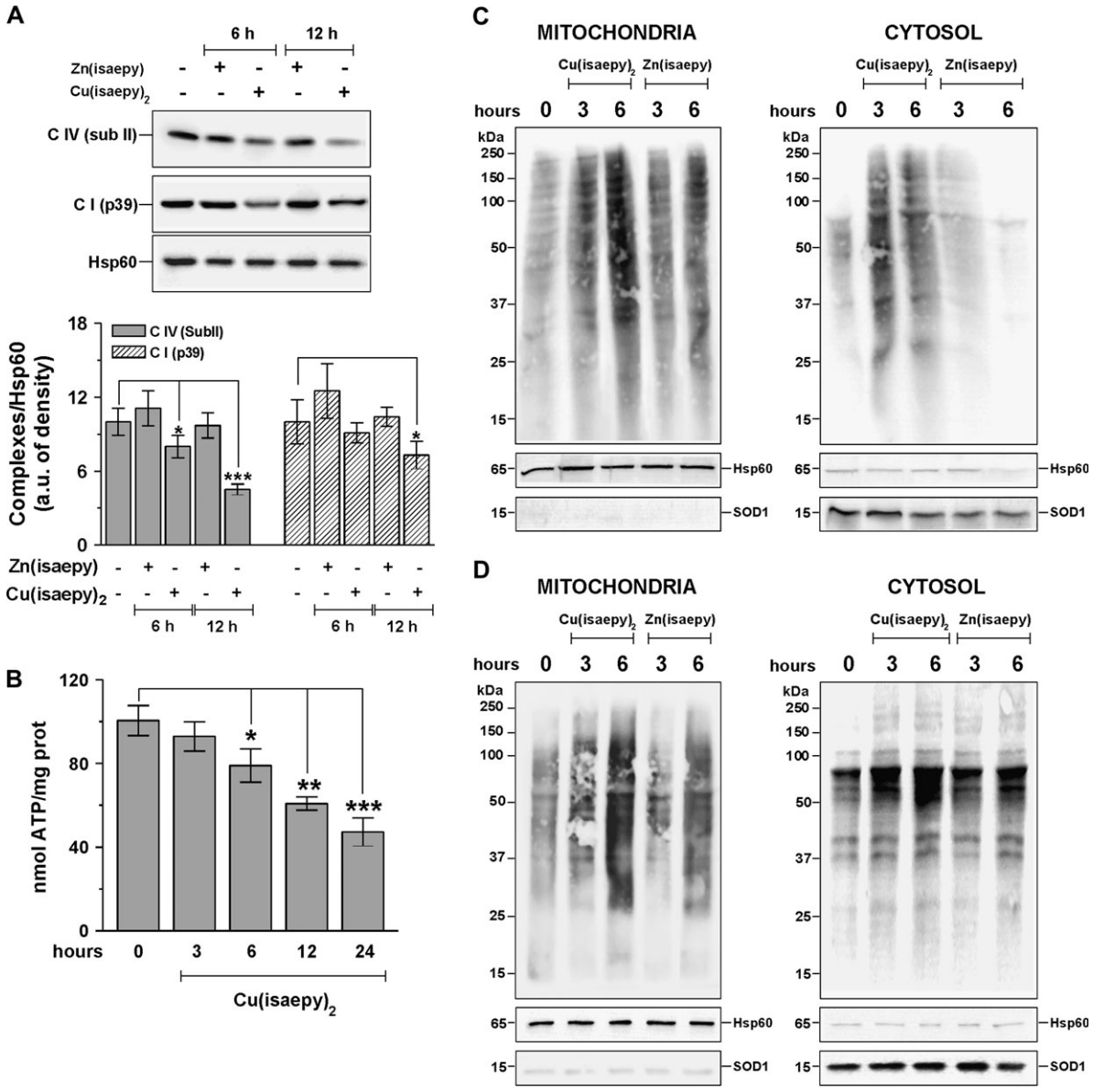

Fig. 2. Structural/functional alterations in mitochondria of $Cu(isaepy)_2$-treated SH-SY5Y cells. (**A**) SH-SY5Y cells were treated for 6 and 12 h with 50 μM $Cu(isaepy)_2$ or Zn(isaepy). Fifteen microgams of mitochondrial protein extracts were loaded onto each lane for detection of subunit II of cytochrome *c* oxidase, C IV (sub II) and 39 kDa subunit of Complex I, C I (p39). Hsp60 was used as loading/purity control and densitometry of each lane (bottom panel) was calculated using Quantity One Software [gray bars, C IV (sub II); striped bars, C I (p39)]. Data are expressed as arbitrary units with respect to Hsp60 and represent the mean ± SD of $n = 4$ independent experiments, $^{*}P < 0.05$, $^{***}P < 0.001$. (**B**) SH-SY5Y cells were treated with 50 μM $Cu(isaepy)_2$. At indicated times, cells were harvested and used for ATP measurement. Data are expressed as percentage of control and represent the mean ± SD of $n = 12$ independent experiments, $^{*}P < 0.05$; $^{**}P < 0.01$ and $^{***}P < 0.001$. SH-SY5Y cells were treated for 3 and 6 h with 50 μM $Cu(isaepy)_2$ or Zn(isaepy) in the absence (**C**) or in the presence (**D**) of 10 μM of the proteasome inhibitor, MG132. Ten microgams of mitochondrial proteins and 25 μg of cytosolic proteins were reacted with 2,4-dinitrophenylhydrazine (DNP), resolved on 8.5% sodium dodecyl sulfate–polyacrylamide gel electrophoresis and DNP-derivatized proteins identified by western blot using an anti-DNP antibody. SOD1 and Hsp60 were used as loading/purity controls.

mitochondrial extracts, while being efficiently buffered in the cytosol. To verify whether the latter process was dependent on the cytosolic activation of proteasome, we pretreated the cells with 10 μM of the proteasome inhibitor, MG132, and then analyzed the level of carbonylated proteins. Figure 2D shows that, by inhibiting the proteasome, no significant change of mitochondrial carbonyls was observed. On the

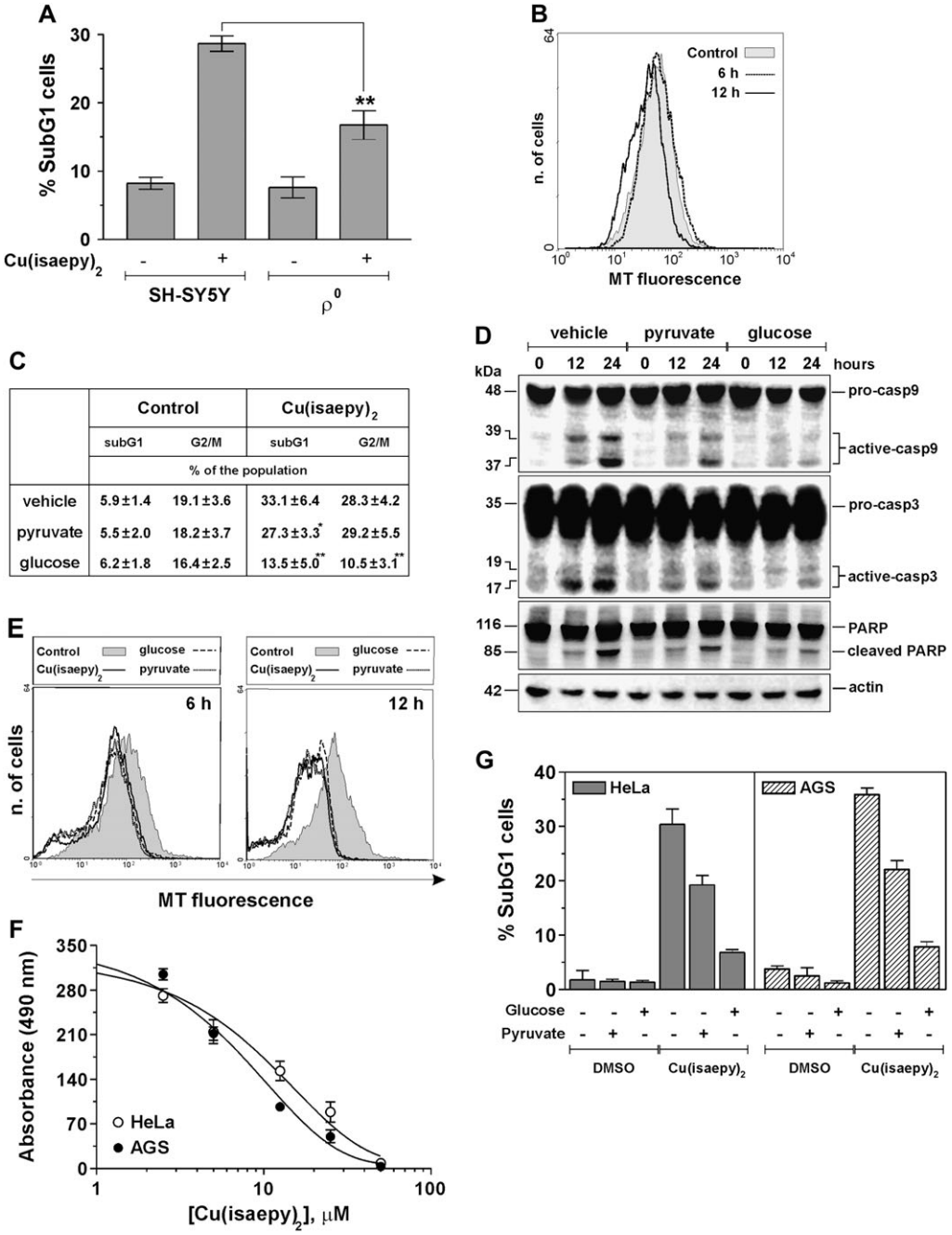

Fig. 3. Effect of glucose or pyruvate supplementation on Cu(isaepy)$_2$-induced apoptosis. (**A**) SH-SY5Y and mitochondrial DNA-devoid ρ^0 cells were treated for 24 h with 50 μM Cu(isaepy)$_2$ and cytofluorometrically analyzed for apoptosis extent. Data are expressed as percentage of SubG$_1$ cells and represent the mean ± SD of $n = 3$ independent experiments, $^{**}P < 0.01$. (**B**) ρ^0 Cells were treated for 6 and 12 h with 50 μM Cu(isaepy)$_2$, incubated for 30 min with 50 nM MitoTracker Red (MT) and cytofluorometrically analyzed for $\Delta\Psi_m$ by FACScalibur instruments. Histograms shown are representative of three experiments that gave similar results. (**C**) SH-SY5Y cells were treated for 24 h with 50 μM Cu(isaepy)$_2$ in the presence of 30 mM glucose or 10 mM sodium pyruvate and cytofluorometrically analyzed for the extent of G$_2$/M as well as SubG$_1$ (apoptotic) cells. Data are expressed as percentage of the total population and represent the mean ± SD of $n = 4$ independent experiments, $^{*}P < 0.05$, $^{**}P < 0.01$. (**D**) SH-SY5Y cells were treated for 12 and 24 h with 50 μM Cu(isaepy)$_2$ in the presence of 30 mM glucose or 10 mM sodium pyruvate. Thirty micrograms of proteins from total cell lysates were loaded onto each lane for the detection of pro and active caspase-9, pro and active caspase-3 and poly(ADP-ribose) polymerase. Actin was used as loading control. (**E**). SH-SY5Y cells were treated for 6 and 12 h with 50 μM Cu(isaepy)$_2$ in the presence of 30 mM glucose or 10 mM sodium pyruvate, incubated for 30 min with 50 nM MitoTracker Red (MT) and cytofluorometrically analyzed for $\Delta\Psi_m$ by FACScalibur instruments. Histograms shown are representative of three experiments that gave similar results. (**F**). Gastric and cervix adenocarcinoma AGS and HeLa cells were incubated for 24 h with different concentrations of Cu(isaepy)$_2$ ranging from 2.5 to 50 μM and evaluated by an 3-(4,5-dimethylthiazol-2-yl)-5-(3-carboxymethoxyphenyl)-2-(4-sulfophenyl)-2H-tetrazolium inner salt assay. Data are expressed as absorbance units at 490 nm and represent the mean ± SD of $n = 12$ experiments. (**G**) AGS and HeLa cells were treated for 24 h with 10 μM Cu(isaepy)$_2$ in the presence of 30 mM glucose or 10 mM sodium pyruvate and cytofluorometrically analyzed for apoptosis extent. Data are expressed as percentage of SubG$_1$ cells and represent the mean ± SD of $n = 3$ independent experiments.

contrary, a time-dependent accumulation of cytosol-sited carbonylated proteins was determined (supplementary Figure 3A and B is available at *Carcinogenesis* Online), confirming the prominent role of proteasome machinery in clearing oxidized proteins in the cytosolic compartment.

Increased glycolytic rate counteracts Cu(isaepy)$_2$-induced apoptosis, but not $\Delta\Psi_m$ loss

The results obtained suggest that mitochondrial damage is causal of Cu(isaepy)$_2$-mediated apoptosis. Therefore, we generated ρ^0 cells that lack mitochondrial transport chain (15). Then, we treated the cells with Cu(isaepy)$_2$ for 24 h and analyzed cytofluorometrically the percentage of apoptotic cells. Figure 3A shows that ρ^0 cells were more resistant to Cu(isaepy)$_2$ with respect to parental SH-SY5Y. It has been reported that ATP production of ρ^0 cells mainly comes from an efficient glycolysis, which also ensures a proper $\Delta\Psi_m$ (19,20). Figure 3B shows that $\Delta\Psi_m$ of ρ^0 cells was unaffected upon 6 and 12 h treatment with Cu(isaepy)$_2$, in line with the observed increased resistance to Cu(isaepy)$_2$ toxicity.

To evaluate to which extent glycolysis could counteract Cu(isaepy)$_2$-induced cytotoxicity, we supplemented cell medium of SH-SY5Y with glucose up to a concentration of 30 mM. Alternatively, we added 10 mM sodium pyruvate to supply the electron transfer chain with reducing equivalents, avoiding glycolysis. Figure 3C shows that glucose addition made the cells more resistant to both cell cycle arrest in G_2/M phase and apoptosis induced by 24 h treatment with 50 μM Cu(isaepy)$_2$. The incubation with pyruvate, instead, produced only a slight protective effect on subG$_1$ cell population. We next analyzed both $\Delta\Psi_m$ and markers of the mitochondrial apoptotic pathway. Figure 3D shows that, upon 24 h treatment with Cu(isaepy)$_2$, cleavage of either caspase-9 or caspase-3 as well as poly(ADP-ribose) polymerase was slightly attenuated upon pyruvate addition. In contrast, it appeared to be almost completely abolished upon glucose supplementation, confirming that an increased rate of the glycolytic pathway was protective. However, this protection was not paralleled by a recovery of $\Delta\Psi_m$ (Figure 3E), which, instead, decreased similarly to what observed upon treatment with Cu(isaepy)$_2$ under basal conditions.

Carcinoma cells are known to rely most of their ATP production on mitochondrial oxidative phosphorylation (21), representing, for this reason, the elective tumor histotypes for DLCs-based chemotherapy (6). Therefore, we assess the effectiveness of Cu(isaepy)$_2$ in cervix (HeLa) and gastric (AGS) adenocarcinoma cells. Figure 3F shows the dose-response profile obtained for these cells with the IC$_{50}$ values of 10.5 ± 1.2 and 7.3 ± 0.9 μM for HeLa and AGS, respectively. Moreover, Figure 3G shows that treatment of AGS and HeLa cells with 10 μM Cu(isaepy)$_2$ resulted in apoptosis that was significantly inhibited by glucose supplementation.

AMPK regulates cell sensitivity to Cu(isaepy)$_2$

In parallel to the characterization of the effect of Cu(isaepy)$_2$ on mitochondrial homeostasis, we investigated its effect on cell signaling. It has been reported that AMPK is an early sensor of energetic impairment, as well as it rapidly activates in response to genotoxic stress. Therefore, we wondered whether AMPK was activated under our experimental conditions. Figure 4A shows that phospho-AMPK, which represents the active form of the enzyme, rapidly increased

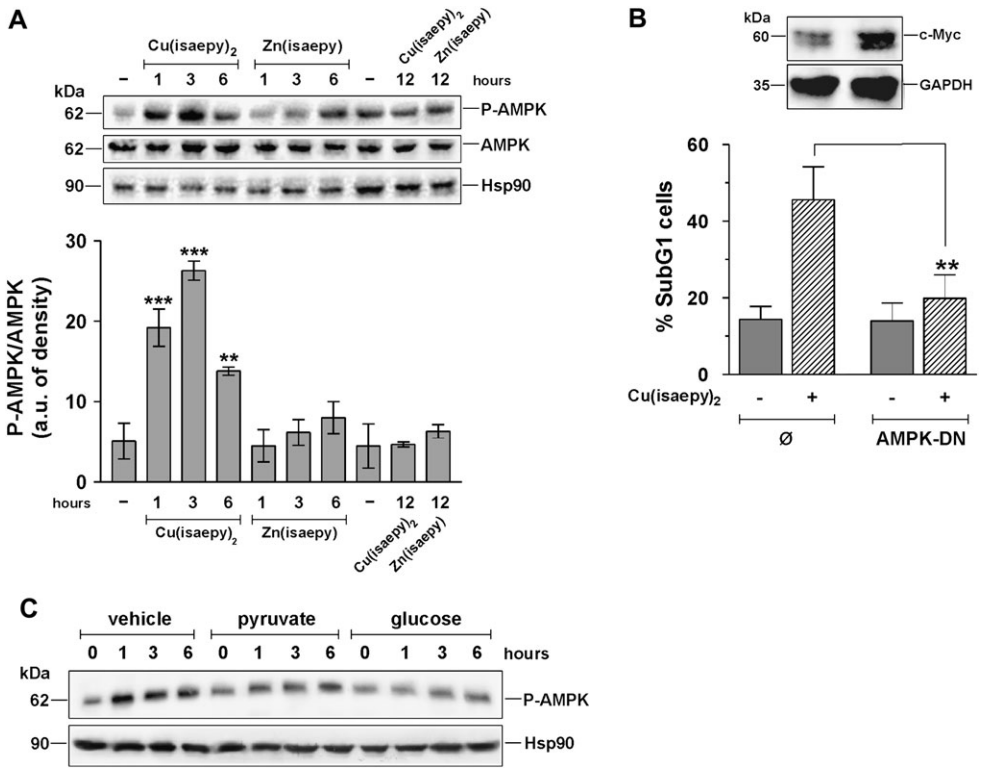

Fig. 4. Effect of Cu(isaepy)$_2$ on downstream signaling leading to apoptosis. (**A**) SH-SY5Y cells were treated with 50 μM Cu(isaepy)$_2$ or Zn(isaepy). At each time point, 15 μg of proteins from total cell lysates was loaded onto each lane for the detection of the basal and phospho-active AMPK. Hsp90 was used as loading control and densitometry of each lane (bottom panel) was calculated using Quantity One Software. Data are expressed as arbitrary units of phospho/basal AMPK and represent the mean ± SD of $n = 3$ independent experiments, $^{**}P < 0.01$; $^{***}P < 0.001$. (**B**) SH-SY5Y cells were transfected with an empty pcDNA vector (Ø) or with a pcDNA vector containing the myc-tagged T172A non-phosphorylable form of AMPK (AMPK-DN). After 24 h treatment with 50 μM Cu(isaepy)$_2$, the efficiency of transfection was evaluated by the immune detection of c-myc, whereas glyceraldehyde-3-phosphate dehydrogenase (GAPDH) was used as loading control (upper panel). Concomitantly, cells were cytofluorometrically analyzed for apoptosis extent (bottom panel). Data are expressed as percentage of SubG$_1$ cells and represent the mean ± SD of $n = 4$ independent experiments, $^{**}P < 0.01$. (**C**) SH-SY5Y cells were incubated with 30 mM glucose or 10 mM sodium pyruvate and treated with 50 μM Cu(isaepy)$_2$. At each time point, 15 μg of proteins from total cell lysates was loaded onto each lane for the detection of phospho-active AMPK. Hsp90 was used as loading control.

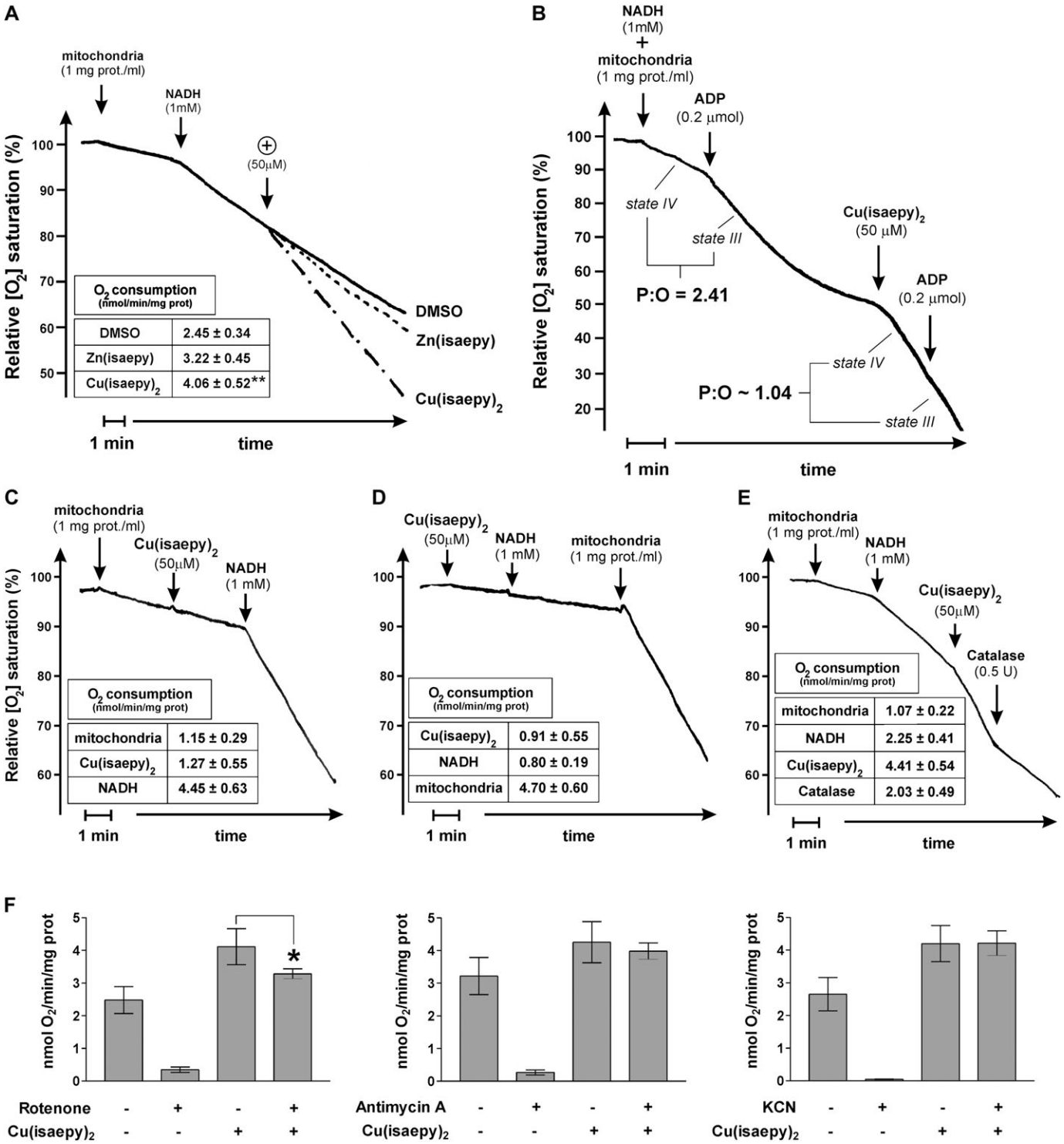

Fig. 5. Effect of Cu(isaepy)$_2$ on isolated mitochondria. Purified mitochondria from mouse liver were used to measure oxygen consumption by a Clark-type oxygen electrode maintained at 25°C. (**A**) Cu(isaepy)$_2$ affects oxygen consumption. In total, 1 mM NADH, 50 μM Cu(isaepy)$_2$, 50 μM Zn(isaepy) or dimethyl sulfoxide (DMSO) (equal volumes) were added to mitochondria sequentially, as indicated. Trace shown is from one representative experiment out of 10 that gave similar results. Data are expressed in the bottom table as nanomoles of O_2 consumed·per minute per milligram protein and represent the mean ± SD of $n = 8$ independent experiments, $^{**}P < 0.01$. (**B**) Cu(isaepy)$_2$ affects state III:state IV ratio. Trace shown and P:O values are from one representative experiment out of five that gave similar results. (**C**) Cu(isaepy)$_2$ affects oxygen consumption in the presence of NADH. Trace shown is from one representative experiment out of five that gave similar results. Data are expressed in the bottom table as nanomoles of O_2 consumed·per minute per milligram protein and represent the mean ± SD of $n = 3$ independent experiments. (**D**). Cu(isaepy)$_2$ affects oxygen consumption in the presence of NADH and mitochondria. Trace shown is from one representative experiment out of five that gave similar results. Data are expressed in the bottom table as nanomoles of O_2 consumed per minute per milligram protein and represent the mean ± SD of $n = 3$ independent experiments. (**E**) Cu(isaepy)$_2$ induces ROS production. In total, 0.5 U catalase were added to mitochondria. Trace shown is from one representative experiment out of seven that gave similar results. Data are expressed in the bottom table as nanomoles of O_2 consumed·per minute per milligram protein and represent the mean ± SD of $n = 5$ independent experiments. (**F**) Cu(isaepy)2 affects Complex I activity. In total, 5 μM rotenone, 5 μM antimycin A and 1 mM KCN were added to mitochondria. Data are expressed as nanomoles of O_2 consumed per minute per milligram protein and represent the mean ± SD of $n = 5$ independent experiments, $^{*}P < 0.05$.

upon treatment with 50 μM Cu(isaepy)$_2$, whereas only slight effects were evidenced upon treatment with 50 μM Zn(isaepy). To unravel the role of AMPK in the induction of apoptosis, we transfected the cells with a pcDNA3 vector containing the myc-tagged non-phosphorylable dominant/negative form (T172A) of the α2 subunit of AMPK (AMPK-DN cells) and treated them with Cu(isaepy)$_2$ for 24 h. The efficiency of transfection was determined by western blot analyses against c-myc (inset Figure 4B). Figure 4B also shows that the percentage of apoptosis was significantly lowered by the inhibition of AMPK, clearly indicating its involvement in the apoptotic response against energetic stress mediated by Cu(isaepy)$_2$. Moreover, Figure 4C shows that pyruvate, but mostly glucose, produced a significant inhibition of AMPK phospho-activation. Similar results were also obtained with ρ^0 cells (data not shown).

Cu(isaepy)$_2$ increases NADH-dependent oxygen consumption of isolated mitochondria independent on ADP

Finally, we aimed at characterizing the site of action of Cu(isaepy)$_2$ onto mitochondria. We then purified mitochondria from mouse liver and measured NADH-dependent oxygen consumption upon incubation with 50 μM of both Cu(isaepy)$_2$ and Zn(isaepy). Figure 5A shows that only Cu(isaepy)$_2$ significantly increased oxygen consumption of ∼60% with respect to mitochondria (1 mg/ml) incubated with vehicle alone; conversely, succinate-dependent respiration was completely unaffected (data not shown). To assess whether ADP could influence Cu(isaepy)$_2$-mediated effects, we measured state III:state IV ratio. Figure 5B shows that, in the presence of Cu(isaepy)$_2$, oxygen consumption was insensitive to ADP addition. In particular, P:O decreased to values close to 1, indicating that Cu(isaepy)$_2$ behaved as an uncoupling molecule.

Next, isolated mitochondria were incubated with Cu(isaepy)$_2$ in the absence of NADH. These experiments were performed either in the presence or absence of glutamate and malate. Figure 5C shows that, under these conditions, Cu(isaepy)$_2$ was completely ineffective in increasing oxygen consumption, which, instead, was rapidly induced upon the addition of NADH. The phenomenon observed was not dependent on unspecific reactions since increased oxygen consumption by Cu(isaepy)$_2$ was observed only in the presence of mitochondria and NADH (Figure 5D).

Therefore, in order to assess whether Cu(isaepy)$_2$-mediated NADH oxidation could be responsible for ROS generation, mitochondria were incubated with Cu(isaepy)$_2$ in experimental buffer containing glutamate/malate and NADH in the presence of 0.5 U of catalase. Figure 5E shows that the addition of catalase halved oxygen consumption, indicating that Cu(isaepy)$_2$ dissipates NADH-deriving reducing equivalents to form O_2^-/H_2O_2. We then evaluated which Complex was involved in the increased oxygen consumption by Cu(isaepy)$_2$. To this aim, isolated mitochondria were incubated with Cu(isaepy)$_2$ in the presence of rotenone, antimycin A or KCN, which inhibit irreversibly Complex I, III and IV, respectively. Figure 5F shows that rotenone was the sole inhibitor able to influence the increase of oxygen consumption induced by Cu(isaepy)$_2$ (−18%), implying a direct, although not principal, involvement of Complex I in this phenomenon.

Discussion

In the present study, we have deeply investigated the mitochondriotoxic action of Cu(isaepy)$_2$ and clarified the mechanisms responsible for the final induction of apoptosis (see scheme in Figure 6) further validating the specific role of mitochondria in Cu(isaepy)$_2$-mediated antiproliferative effects. We demonstrated that Cu(isaepy)$_2$ increases oxygen consumption in a way similar to that occurring with uncoupling molecules. Specifically, our results provide evidence for the partial reduction of oxygen to generate ROS, rather than being engaged as the ultimate sink of the tetravalent reduction mediated by the electron transfer chain. Such observation comes from experiments carried out with purified mitochondria incubated with Cu(isaepy)$_2$,

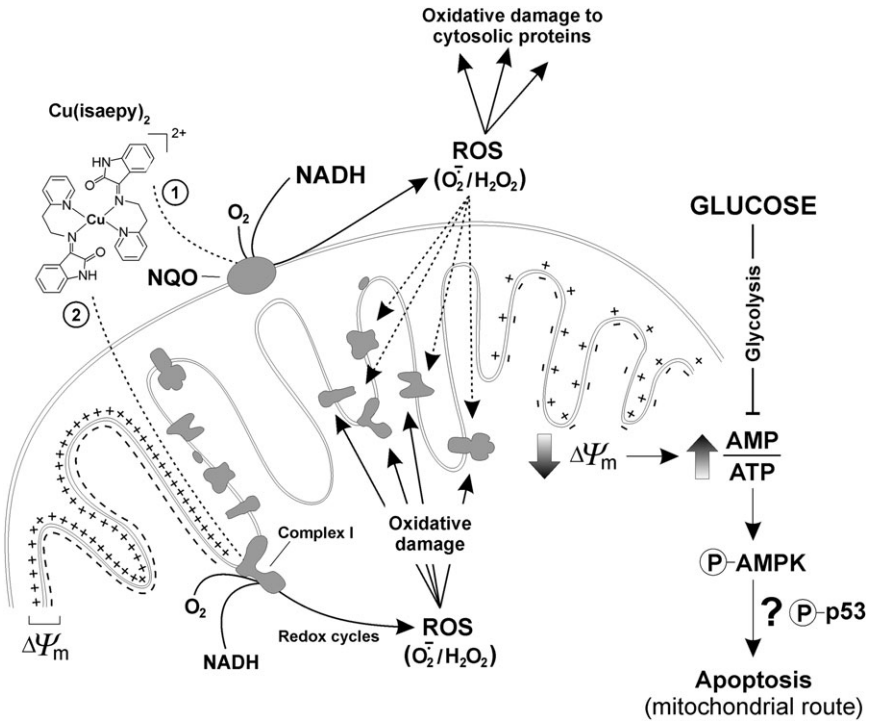

Fig. 6. Schematic representation of the effects of Cu(isaepy)$_2$. Cu(isaepy)$_2$ behaves as a DLC-like molecule preferentially targeting mitochondria. In particular, we proposed that Cu(isaepy)$_2$ reacts with NADH mainly by means of mitochondrial NADH:quinone oxidoreductases (NQO) sited at the outer membrane (pathway 2), but also through Complex I (pathway 1). The resulting copper-catalyzed redox cycles lead to ROS generation and to a widespread oxidative damages to proteins, above all those contained in the mitochondrial compartment. Such general dysfunction produces $\Delta\Psi_m$ loss and ATP decrease, which in turn triggers the phospho-activation of AMPK and the consequent induction of the mitochondrial pathway of apoptosis.

which clearly point out that oxygen consumption is completely independent on ADP addition, as well as strongly reduced by catalase. The pro-oxidant activity of Cu(isaepy)$_2$ has been also confirmed in cell systems to be mitochondrion specific. In fact, the analysis of carbonylated proteins, one of the most common oxidative modifications of proteins, shows that they accumulate in mitochondrial extracts, whereas seem to be efficiently scavenged within the cytosol by a proteasome-dependent degradation process. These results are confirmatory of a persistent damage to mitochondria and correlate with the current knowledge that proteasome-dependent degradation efficiently takes place only in the cytosol and the nucleus (22,23). The observed decrement in the levels of respiratory Complexes provides a strong evidence for the mitochondrial specificity of Cu(isaepy)$_2$-mediated oxidative damage. In fact, the decrease of Complex I and IV, which we detected by western blot, represents a hallmark of oxidative damage to mitochondria. Similar results were previously reported to occur upon copper intoxication (24), and it is now well established that mitochondrial Complexes are particularly sensitive to oxidative damages (25,26).

The experiments carried out with purified mitochondria evidenced that oxygen consumption and ROS production were strictly dependent on exogenous NADH availability and generally unaffected by mitochondrial Complexes inhibitors. This suggests that Cu(isaepy)$_2$-catalyzed redox cycles could occur with enzymes other than the electron transfer chain, such as the NADH:quinone oxidoreductases sited at the outer mitochondrial membrane. Indeed, the role of NADH:quinone oxidoreductases in exacerbating the toxicity of diverse DLC classes is now emerging as pivotal for DLCs to produce ROS and selectively target mitochondria of malignant cells (27–30). However, data obtained with rotenone demonstrated that Complex I activity is also affected by Cu(isaepy)$_2$, suggesting that this Complex could be involved in Cu(isaepy)$_2$-mediated mitochondriotoxicity.

Overall, the data indicate that Cu(isaepy)$_2$ can be included among DLCs. Such assumption also originates from the evidence that: (i) $\Delta\Psi_m$ drop is tightly associates with a rapid decrease of ATP levels and insensitive to glucose supplementation; (ii) glucose addition to culture media prevents or, at least, strongly delays Cu(isaepy)$_2$-mediated cell death and (iii) carcinoma HeLa and AGS cell lines, which are known to rely most of their energy production upon mitochondrial oxidative phosphorylation, are much more susceptible toward the toxic effects of Cu(isaepy)$_2$.

In the cascade of events starting from oxidative stress and culminating in apoptosis, we also attempted at identifying the molecular factors involved in the transduction pathways of apoptotic signal. In particular, we have investigated the involvement of AMPK as a component of such cascade that are able to sense the upstream energetic stress and responsible for the downstream induction of apoptosis. AMPK is now emerging as modulator of different cellular responses, all converging in the restoration of ATP levels (31–33). However, it can also phospho-activate many proteins involved in the induction of apoptosis, such as some members of the mitogen-activated protein kinase family (e.g. p38^{MAPK}) (34) or p53 (35,36), representing in such a way a crossroad between survival and death. In this work, we have demonstrated that AMPK is responsible for Cu(isaepy)$_2$-induced apoptosis since the overexpression of the non-phosphorylable T172A form of the α2 subunit of the enzyme completely rescues cells from death. Previously, we reported that p53 was involved in Cu(isaepy)$_2$-induced apoptosis (14); therefore, on the basis of the results obtained here, we can hypothesize a molecular link between AMPK and p53 and a functional synergism between them in apoptosis occurrence. Work is in progress in our laboratory aimed at investigating the possible involvement of a cross talk between these two proteins in the induction of Cu(isaepy)$_2$-mediated apoptosis and whether the activation of other protein kinases, such as p38^{MAPK}, is implicated in such phenomenon. The results emerging from this study are promising and useful to outline a programmed transduction pathway downstream of Cu(isaepy)$_2$, rather than considering this compound only as a copper delivery molecule able to produce widespread cell dysfunction as downstream effect of metal intoxication. In such a way, Cu(isaepy)$_2$ could be proposed for its putative use as a novel DLC compound useful in *in vivo* approaches for cancer treatment.

Supplementary material

Supplementary Figures 1–3 can be found at http://carcin.oxfordjournals.org/

Funding

Ministero della Salute; Ministero dell'Istruzione, dell'Università e della Ricerca; Fondo per gli Investimenti della Ricerca di Base 'Idee Progettuali'.

Acknowledgements

We gratefully acknowledge Dr Palma Mattioli for her assistance in microscopy and image analyses.

Conflict of Interest Statement: None declared.

References

1. Griffiths,J.R. (2001) Causes and consequences of hypoxia and acidity in tumour microenvironments. *Bioessays*, **23**, 295–296.
2. Bernal,S.D. *et al*. (1983) Anticarcinoma activity *in vivo* of rhodamine 123, a mitochondrial-specific dye. *Science*, **222**, 169–172.
3. Geschwind,J.F. *et al*. (2002) Novel therapy for liver cancer: direct intraarterial injection of a potent inhibitor of ATP production. *Cancer Res.*, **62**, 3909–3913.
4. Ko,Y.H. *et al*. (2004) Advanced cancers: eradication in all cases using 3-bromopyruvate therapy to deplete ATP. *Biochem. Biophys. Res. Commun.*, **324**, 269–275.
5. Maher,J.C. *et al*. (2004) Greater cell cycle inhibition and cytotoxicity induced by 2-deoxy-D-glucose in tumor cells treated under hypoxic vs aerobic conditions. *Cancer Chemother. Pharmacol.*, **53**, 116–122.
6. Murphy,M.P. (2004) Investigating mitochondrial radical production using targeted probes. *Biochem. Soc. Trans.*, **32**, 1011–1014.
7. Modica-Napolitano,J.S. *et al*. (2001) Delocalized lipophilic cations selectively target the mitochondria of carcinoma cells. *Adv. Drug Deliv. Rev.*, **49**, 63–70.
8. Modica-Napolitano,J.S. *et al*. (1987) Basis for the selective cytotoxicity of rhodamine 123. *Cancer Res.*, **47**, 4361–4365.
9. Sun,X. *et al*. (1994) AA1, a newly synthesized monovalent lipophilic cation, expresses potent *in vivo* antitumor activity. *Cancer Res.*, **54**, 1465–1471.
10. Anderson,W.M. *et al*. (1993) Cytotoxic effect of thiacarbocyanine dyes on human colon carcinoma cells and inhibition of bovine heart mitochondrial NADH-ubiquinone reductase activity via a rotenone-type mechanism by two of the dyes. *Biochem. Pharmacol.*, **45**, 691–696.
11. Weiss,M.J. *et al*. (1987) Dequalinium, a topical antimicrobial agent, displays anticarcinoma activity based on selective mitochondrial accumulation. *Proc. Natl Acad. Sci. USA*, **84**, 5444–5448.
12. Modica-Napolitano,J.S. *et al*. (1996) Selective damage to carcinoma mitochondria by the rhodacyanine MKT-077. *Cancer Res.*, **56**, 544–550.
13. Koya,K. *et al*. (1996) MKT-077, a novel rhodacyanine dye in clinical trials, exhibits anticarcinoma activity in preclinical studies based on selective mitochondrial accumulation. *Cancer Res.*, **56**, 538–543.
14. Filomeni,G. *et al*. (2007) Pro-apoptotic activities of novel Isatin-Schiff base copper(II) complexes depends on oxidative stress induction and organelle-selective damage. *J. Biol. Chem.*, **282**, 12010–12021.
15. Miller,S.W. *et al*. (1996) Creation and characterization of mitochondrial DNA-depleted cell lines with ''neuronal-like'' properties. *J. Neurochem.*, **67**, 1897–1907.
16. Lowry,O.H. *et al*. (1951) Protein measurement with the Folin phenol reagent. *J. Biol. Chem.*, **193**, 265–275.
17. Benard,G. *et al*. (2008) Ultrastructure of the mitochondrion and its bearing on function and bioenergetics. *Antioxid. Redox Signal.*, **10**, 1313–1342.
18. Rae,T.D. *et al*. (1999) Undetectable intracellular free copper: the requirement of a copper chaperone for superoxide dismutase. *Science*, **284**, 748–749.
19. Buchet,K. *et al*. (1998) Functional F1-ATPase essential in maintaining growth and membrane potential of human mitochondrial DNA-depleted rho degrees cells. *J. Biol. Chem.*, **273**, 22983–22989.
20. Arnould,T. *et al*. (2003) mtCLIC is up-regulated and maintains a mitochondrial membrane potential in mtDNA-depleted L929 cells. *FASEB J.*, **17**, 2145–2147.

21. Rodríguez-Enríquez,S. *et al*. (2006) Control of cellular proliferation by modulation of oxidative phosphorylation in human and rodent fast-growing tumor cells. *Toxicol. Appl. Pharmacol.*, **215**, 208–217.
22. Davies,K.J. (2001) Degradation of oxidized proteins by the 20S proteasome. *Biochimie*, **83**, 301–310.
23. Grune,T. *et al*. (2003) Selective degradation of oxidatively modified protein substrates by the proteasome. *Biochem. Biophys. Res. Commun.*, **305**, 709–718.
24. Arciello,M. *et al*. (2004) Copper-dependent toxicity in SH-SY5Y neuroblastoma cells involves mitochondrial damage. *Biochem. Biophys. Res. Commun.*, **327**, 454–459.
25. Halliwell,B. *et al*. (1990) Role of free radicals and catalytic metal ions in human disease: an overview. *Methods Enzymol.*, **186**, 1–85.
26. Cadenas,E. *et al*. (2000) Mitochondrial free radical generation, oxidative stress, and aging. *Free Radic. Biol. Med.*, **29**, 222–230.
27. Spanswick,V.J. *et al*. (1996) Enzymology of mitomycin C metabolic activation in tumour tissue. Characterization of a novel mitochondrial reductase. *Biochem. Pharmacol.*, **51**, 1623–1630.
28. Shimada,H. *et al*. (1998) Mitochondrial NADH-quinone oxidoreductase of the outer membrane is responsible for paraquat cytotoxicity in rat livers. *Arch. Biochem. Biophys.*, **351**, 75–81.
29. Liochev,S.I. *et al*. (1998) Lucigenin as mediator of superoxide production: revisited. *Free Radic. Biol. Med.*, **25**, 926–928.
30. Kruglov,A.G. *et al*. (2007) The effect of the lipophilic cation lucigenin on mitochondria depends on the site of its reduction. *Biochem. Pharmacol.*, **74**, 545–556.
31. Carling,D. (2004) The AMP-activated protein kinase cascade-a unifying system for energy control. *Trends Biochem. Sci.*, **29**, 18–24.
32. Towler,M.C. *et al*. (2007) AMP-activated protein kinase in metabolic control and insulin signaling. *Circ. Res.*, **100**, 328–341.
33. Hardie,D.G. (2007) AMP-activated/SNF1 protein kinases: conserved guardians of cellular energy. *Nat. Rev. Mol. Cell Biol.*, **8**, 774–785.
34. Cao,C. *et al*. (2008) AMP-activated protein kinase contributes to UV- and H2O2-induced apoptosis in human skin keratinocytes. *J. Biol. Chem.*, **283**, 28897–28908.
35. Jones,R.G. *et al*. (2005) AMP-activated protein kinase induces a p53-dependent metabolic checkpoint. *Mol. Cell*, **18**, 283–293.
36. Okoshi,R. *et al*. (2008) Activation of AMP-activated protein kinase induces p53-dependent apoptotic cell death in response to energetic stress. *J. Biol. Chem.*, **283**, 3979–3987.

Received January 15, 2009; revised March 31, 2009; accepted April 25, 2009